Article:
Shi, J, Zhang, F, Wu, S et al. (5 more authors) (2019) Noise-free microbial colony counting method based on hyperspectral features of agar plates. Food Chemistry, 274. pp. 925-932. ISSN 0308-8146

https://doi.org/10.1016/j.foodchem.2018.09.058

Noise-free microbial colony counting method for food quality assessment using hyperspectral features

Jiyong Shi[a, c], Fang Zhang[a], Shengbin Wu[a], Xuetao Hu[a], Xiaobo Zou[a, c, *] Mel Holmes[b,c], Xiaowei Huang[a], Zhiming Guo[a]

[a] School of Food and Biological Engineering, Jiangsu University, Zhenjiang 212013, China

[b] School of Food Science and Nutrition, the University of Leeds, Leeds LS2 9JT, United Kingdom

[c] Joint Laboratory of China-UK on food nondestructive sensing, Jiangsu University, Zhenjiang 212013, China

[*]Corresponding author. Tel: +86 511 88790958; Fax: +86 511 88780201

Email address: zou_xiaobo@ujs.edu.cn (Xiaobo Zou)

Abstract

A noise-free bacterial colony counting method that can identify noises with similar colors/shapes of colonies was proposed for food quality assessment. Noises were produced using food fragments (sausage, bacon, and millet fragments) sterilized at high temperatures. Agar plates with colonies and food fragments in/on agar medium were used to acquire hyperspectral image data. Firstly, spectral features corresponding to the colony cluster regions and the background regions (agar medium and food fragments) were extracted from hyperspectral images. A cluster segmenting calibration model that is able to identify colony clusters and background regions was developed based on the spectral features. Secondly, spectral features of colony centers and colony borders were extracted. A colony separating calibration model that can separate single colony from clusters (comprised multiple colonies contacting each other) was developed based on the spectral features. Thirdly, each pixel of an agar plate hyperspectral image was identified using the established calibration models, therefore the colonies on the agar plate can be counted. Results shown that the proposed method got good correlation (R^2= 0.9998) with the standard colony count method. The identification of the noises caused by food fragments with similar colors/shapes of colonies is the outstanding performance of the proposed method.

Keywords: colony, counting, hyperspectral imaging technology, noise-free, spectral feature, chemometrics

1 Introduction

The method of colony counting using solid agar plates has been widely employed to quantitatively measure viable microbial cells for food quality assessment[1]. The colony counting method involves smearing the diluted bacterial suspension of food products on solid agar plate[2]. As each viable cell on the plate grows and then forms a single colony, the number of viable microbial cells in food products can be evaluated by counting the colonies[3]. Colony counting provide essential indicators about probiotics that reflect food nutrition, or harmful organisms that affect food safety[4-6]. Actually, many reference methods or national standards concerning food quality related to various organisms is based on this type of colony counting[7-9]. Conventional colony counting is manually performed by well-trained operators, so it is low throughput, laborious and time-consuming in practice[10].

To alleviate the disadvantages associated with manual counting, various automated colony counting methods using computer vision have been proposed[11-13]. Basically, an image capture system were designed to collect a 2-dimensional color or gray-scale images of the agar plate. Then color features or text features of the colony were extracted from the image and employed to distinguish colony cluster from the background, to separate single colony from clusters composed of touching colonies, and to provide the colony counting results automatically. These kind of automated counting methods can obtain good results as long as interference noise, such as various food fragments, do not appear in the agar plate[2,16].

Unfortunately, it is really difficult to prepare pure samples of target cells without containing any food fragments. As a result, the food fragments maybe wrongly identified as normal colony by computer vision. Researchers have reported that it is difficult to prepare pure samples of target microbial cells without residual food fragments[14]. Technicians worked in government institution of Disease Control and Prevention also reported that food fragments appeared at/in agar medium frequently[15]. As the color and shape of food fragments maybe quite similar to that of normal colonies, food fragments are easily wrongly identified as colonies by computer vision, and even by well-trained employees in practice.

Time-lapse imaging technology, and the use of triphenyl tetrazolium chloride (TTC) have been employed to reduce/eliminate the influence of the food fragments with colors similar to that of colonies. Time-lapse imaging technology collects a series of images to record the dynamic growth of colonies from a single-cells. As the signals of food fragments can be captured prior to the colony, so this method is able to clearly distinguish colonies from the food fragments[16]. However, it requires to repeat the image acquisition many times during the colony culture, and a complex plate holder that can automatically transport agar plate from incubation area to the imaging area has to be installed. Researches figured out that TTC can be used as an indicator because only colonies containing living cells can be marked with red color. The use of TTC significantly increases the contrast between the colonies and the background, and segment of colonies becomes pretty much easy[17]. However, GuoMei et al. reported that TTC affected the growth of microbial cells, which indicated errors would be caused by the use of TTC in the stage of colony growth[18].

A new idea, separating colonies from their background based on spectral features caused by changes in chemical composition, was proposed in this study. Many research have demonstrated that spectral features were sensitive to the chemical components of biological samples; and spectral techniques, such as ultraviolet spectrum (UV)[19], visible spectra (VIS)[20], near infrared spectra (NIR)[21] and mid infrared spectra (MIR)[22] have been used for quantitative and qualitative analysis of chemical composition in various biological samples successfully. Obviously, there are changes in the chemical composition between colony area and agar medium, between colony area and food fragments, and between colony center area and colony border area. So it is reasonable that spectral features were employed to identify colonies and the food fragments with colors similar to that of colonies.

In order to carry out the new idea, it is essential to obtain spectral data of the whole agar plate pixel by pixel, so hyperspectral imaging technology was employed to record the whole agar plate pixel by pixel. Unlike conventional spectral technologies relies on spot measurement, such as UV, VIS, NIR and MIR, hyperspectral imaging technology combines conventional spectroscopy and imaging techniques to acquire a spectrum for

each pixel in the 2-dimensional image of an object[23,24]. There is the case in which the chemical composition of the whole sample must to be evaluated, and it is essential to acquire both spectral data and spatial data from the sample surface at the same time. Hyperspectral imaging technology meets these requirements perfectly and has been successfully used for full assessment of chlorophyll, flavonoids, moisture, soluble solids and other chemical composition in various biological samples[25-29]. It is reasonable to assume that the differences in chemical composition caused by colonies, agar medium, and various noise can be characterized by hyperspectral imaging technology.

As mentioned above, this study was aimed at the development of a noise-free, high-precision method for automatic colony counting. The agar plates with colonies and food fragments were employed to acquire hyperspectral image data. Spectral features corresponding to colonies and backgrounds were employed to count colonies automatically. The performance of the proposed method were compared with that of computer vision, and the practical feasibility of the proposed method was also discussed.

2 Materials and methods

2.1 Preparation of agar plates containing colonies and noise

As an initial model system, nonpathogenic *Bacillus Subtilis* (CGMCC 1.8886) was obtained from China General Microbiological Culture Collection Center (Beijing, China). Food fragments of sausage, bacon, and millet (Kaiyuan supermarket in Jiangsu University) with shapes similar to those of colonies were prepared to cause noise in agar plate. After sterilization at high temperatures using an autoclave (DSX-280B,ShangHai Shenan Medical Instrument Factory, China), 15 ml of Luria-Bertani agar medium (1% tryptone, 0.5% yeast extract, 1% NaCl, and 2% agar) maintained at 47 °C was transferred to a petri dish With a diameter of 90 mm, and food fragments were added to the cooled agar medium. So an agar plate with food fragments on/in the agar medium can be obtained. Various dilutions of *B. subtilis* were prepared in Hanks' Balanced Salt Solution, and 100 μL of the diluted bacteria were spotted onto multiple areas of an agar plate. Then agar plates were placed in an incubator (HWHS-150,

Wanfeng Instrument manufacturing Co. Ltd., China) and cultured for 24 h at 37 °C. The agar plates containing clusters of colonies and food fragments in/on the agar medium were prepared for hyperspectral image data collection, as shown in Figure 1.

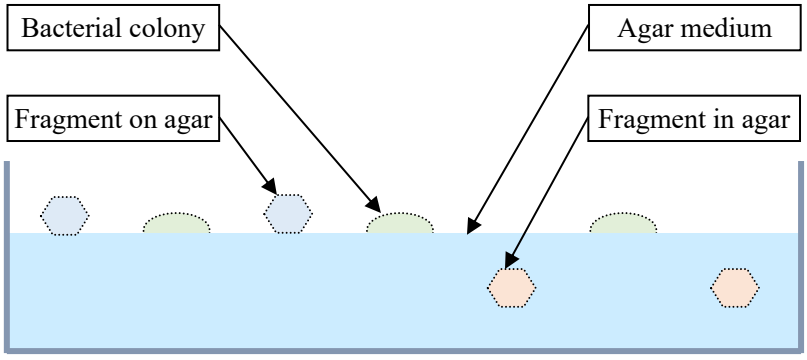

Figure 1 the sectional view of an ager plate with bacterial colonies and food fragments on/in agar medium

2.2 Hyperspectral image data measurement

A line-scanning hyperspectral imaging system with the Vis/Nir wavelength range of 400-1000 nm was employed to acquire hyperspectral images of the prepared agar plates in the reflectance mode. The hyperspectral imaging system consists of a line-scanning spectrograph (ImSpector, VI0E, Spectra Imaging Ltd., Finland), a CMOS camera (BCi4-U-M-20-LP, Vector International, Belgium), a illuminator (Fiber-Lite PL900-A, Dolan-Jenner Industries Inc., USA), a conveyer (Zolix TS200AB, Zolix. Corp., China), an enclosure (ZJgrt, Great Ltd., China), a data acquisition and pre-processing software (Spectra Cube, Auto Vision Inc., USA), and a computer (HPdx2390MT, Hewlett-Packard, China). Detailed information about hyperspectral image collection can be found in our previous study[30].

2.3 Hyperspectral image data analysis

After hyperspectral image measurement, the agar plate was digitized with pixels that contain spectra data, so the spectral features of each pixel can be employed to segment colonies from background and split colony clusters.

With the aid of hyperspectral imaging system, the 3-dimensional (3D) data cube of agar plate was acquired as shown in Fig 2. In Fig. 2 (a), x axis and y axis indicate the pixel location, λ axis indicates the wavelength of every single image. The significant

advantage of the 3D data cube is that it contains both spectral data and image data of an agar plate. On the one hand, the 3D data of an individual pixel (x equals to $x_j \in [1, 1024]$, y equals to $y_k \in [1, 1024]$ and λ equals to all the values in the range of [430，960]) is extracted from the whole 3D data cube as shown in Fig. 2 (b). Then all the signal values of the pixel are presented in a curve in order of their wavelengths, and the spectral information of the pixel (x_j, y_k) can be obtained as shown in Fig. 2 (c). On the other hand, the agar plate image at a specific wavelength $\lambda_r \in [430，960]$ (x equals to all the values in the range of [1, 1024] and y equals to all the values in the range of [1, 1024]) can also be extracted from the 3D data cube as shown in Fig. 2 (d). In fact, the whole surface of the agar plate can be digitized accurately with the aid of the pixels in Fig. 2 (a), and the sample properties at every single pixel can be determined rapidly with the aid of its spectral information. This makes it possible to identify colony areas and background areas using their spectral features.

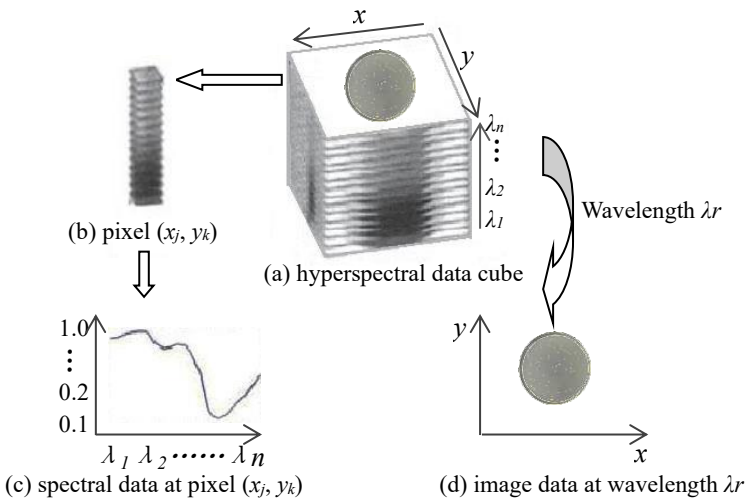

Figure 2 agar plate hyperspectral image data cube

In order to reduce the complexity the hyperspectral data, chemometrics methods were employed to facilitate the establishment of calibration models. Genetic algorithm (GA) is employed to select the most informative wavelength regions from the large hyperspectral image data[31-33], Principal component analysis (PCA) is employed to extract the spectral features from the hyperspectral image data of the selected wavelength regions[34,35], K-nearest neighbors (KNN) is employed to build calibration

models for colony counting[36,37].

2.4 count of microbial colonies

The count of microbial colonies includes three main steps: (1) build cluster segmenting calibration model, (2) build colony separating calibration model, and (3) colony count. The flow chart of these steps is shown in Fig. 3.

2.4.1 Build cluster segmenting calibration model

Firstly, cluster/background spectra were extracted. A square region of interest (ROI) of 10×10 pixels was defined within the cluster and background areas (including agar medium, sausage fragments, bacon fragments, and millet fragments), then the mean spectral data of the cluster and background areas was extracted for further data analysis. Secondly, calibration models for cluster segmentation were build. GA and PCA were used to extract the spectral features of cluster /background pixel from the calibration data set, and KNN was used to build segment models by correlating the spectral features with their origins (cluster area or background area) of pixels. The calibration models were optimized by spectral features of the prediction set. Thirdly, the optimal calibration model was validated by an independent testing data set. The Se and Sp of the predicted results were calculated and were used to estimate the capability of the optimal calibration model.

2.4.2 Build colony separating calibration model

Colony centers are expected to be apart even though the borders of two colonies are contacting each other, so more than 2 colonies overlapping with each other could be counted separately by identifying colony centers. Spectral features of colony centers and colony borders were extracted and employed to build identification models for identifying colony centers, as shown in Fig. 3.

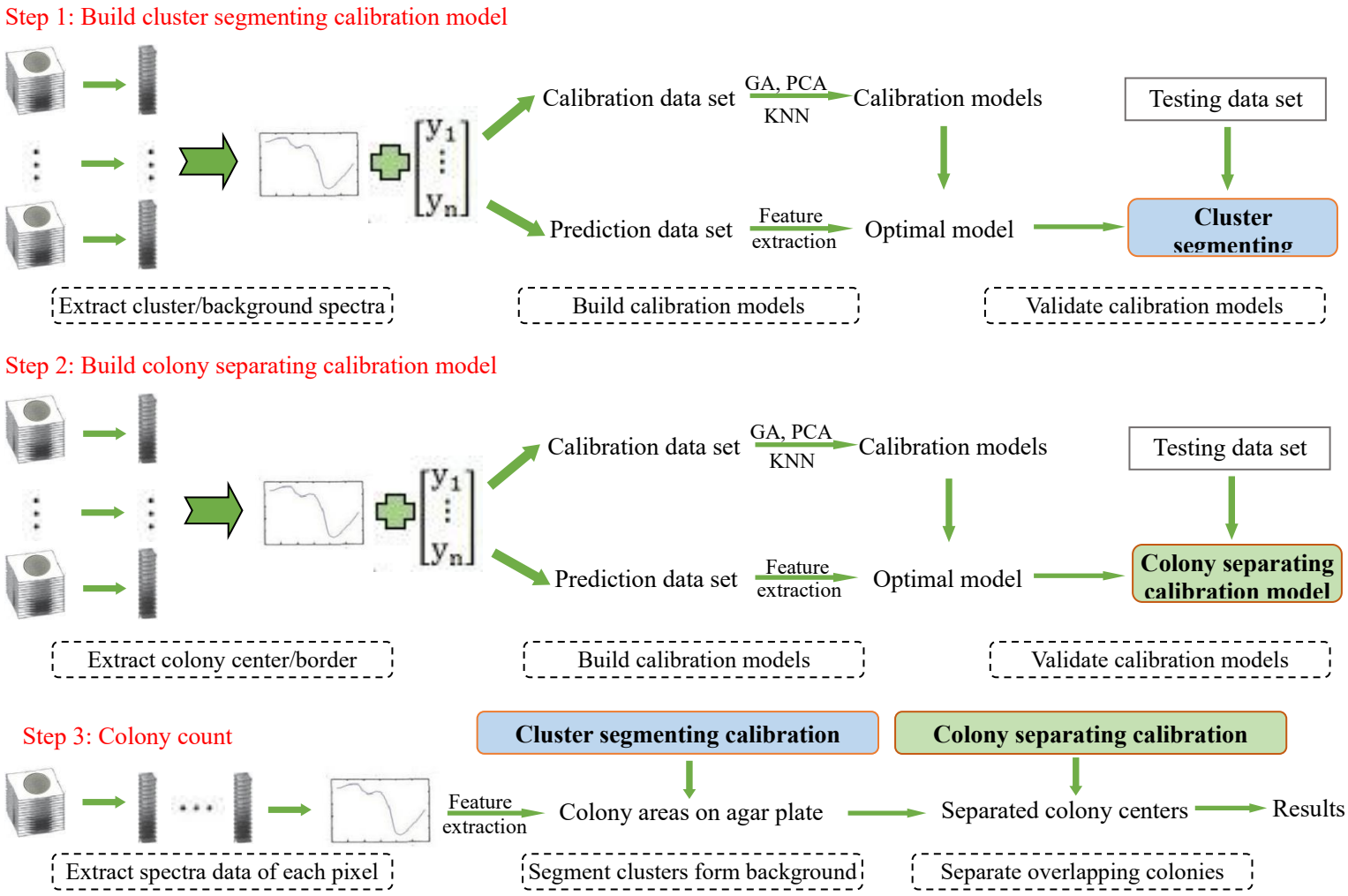

Figure 3 Process flowchart for counting microbial colonies in agar plate

Firstly, colony center/border spectra were extracted. A square region of interest (ROI) of 5×5 pixels was defined within the colony center and border regions in hyperspectral images; then the mean spectral data of the ROI was extracted. Secondly, calibration models for colony separating were build. GA and PCA were used to extract the spectral features of center/border pixel from the calibration data set, and KNN was used to build identification models by correlating the spectral features with their origins (colony center area or colony border area) of pixels. The calibration models were optimized by spectral features of the prediction set. Thirdly, the optimal calibration model was validated by an independent testing data set. The Se and Sp of the predicted results were calculated and were used to estimate the capability of the optimal calibration model.

2.4.3 Colony count

In the cluster segmenting calibration model, the relationship between spectral features and colony/background areas has been established. In the colony separating calibration model, the relationship between spectral features and colony center/border areas has been established. With the aid of the optimal segment model and the optimal identification model, microbial colonies in agar plates can be counted based on the spectral features recorded in the 3D hyperspectral data cube, as show in Fig. 3.

Firstly, spectra data of each pixel in the hyperspectral image of an agar plate with colonies and noises were extracted. Secondly, the cluster areas on the hyperspectral image were segmented. The spectral features of each pixel were substituted in the optimal cluster segmenting calibration model, and then all the pixels were divided into cluster and background areas so that the cluster areas on the agar plate can be segmented. Thirdly, the overlapping colonies were separated. The spectral data of pixels belonging to the cluster areas were substituted in the optimal colony separating calibration model, and then all the pixels were divided into colony center and border

areas so that the colonies contacting with the others can be separated. With the aid of the separated colony centers, all the colonies on the agar plate can be counted. The number of the colony centers was considered as that of colonies in the agar plate due to that each colony own only one colony center.

2.5 Software

The hyperspectral images of agar plates were collected using SpectralCube (ImSpector, image, Auto Vision Inc., USA). All the hyperspectral image processing methods were performed in Matlab V.7.4 (The Mathworks, Natick, USA). The PCA procedure used in this paper is the algorithm contained in Matlab. The source code of the GA algorithm and KNN algorithm was developed based on the demo code presented in the published book[38].

3 results and discussion

3.1 investigation of optical features produced by agar plate

An agar plate containing microbial colonies, sausage/sausage/ millet fragments and agar medium were employed to acquire color image and hyperspectral image, and the spectral/image optical features of colonies and food fragments in color or hyperspectral images were investigated, as shown in Fig. 4.

Computer vision method based on two-dimension images at R/G/B wavelengths has been widely used for colony count, so the color image of the agar plate was collected, as shown in Fig. 4(a). The gray images of the color image at R/G/B wavelengths were shown in Fig. 4(b-c). In Fig. 4(b-c), there is high contrast in gray levels between colonies and agar medium regions and slightly lower contrast between colonies centers and borders. This is agreement with the published papers reporting that colonies can be segment from agar medium with proper threshold gray value while it is difficult to separate single colony from colony clusters using computer vision. In Fig. 4(b-c), it can be also find that gray levels in colony regions are very close to that of food fragment regions, and sometimes the colony region and food

fragment region get the same gray level as marked in the figures. This indicates that it is very difficult to identify colonies from those fragments using conventional color imaging analysis.

The mean spectral data of the colonies and non-colonies particles were extracted from the hyperspectral images of agar plates, as shown in Fig. 4(e). As shown in Fig. 4 (e), the spectral curve of microbial colony is quite different from that of agar medium in the wavelength range of 390-560 nm. The spectral curve of microbial colony and agar medium have similar trends in wavelength range of 610-960 nm, while the spectral readings of microbial colony is different from that of agar medium. In Fig 4(e), it can be also find that the spectral curve of colony is also different from that of food fragments in/on agar medium. Changes in spectral readings and spectral curves are caused by differences in type and quantity of chemical component between colonies and non-colonies particles, as many published papers reported that spectral information is sensitive to chemical components in biochemical samples. This results indicate that changes in spectral reading between colonies and non-colonies particles indicate that spectral features can be employed to segment colonies from its background.

The mean spectral data of colony centers and colony edges were extracted from the hyperspectral images of agar plates, as shown in Fig. 4(f). As shown in Fig. 4 (d), spectral curves of colony centers and colony borders have similar trends in wavelength range of 430-960 nm, the spectral readings of colony centers are different from that of colony edges, especially in the wavelength ranges of 530-570 nm, 730-770 nm and 830-880 nm. Changes in spectral readings are caused by differences in quantity of colony cells between colony centers and colony edges. In fact, differences in quantity of colony cells also cause symmetric gradation of gray levels from the colony border to its center, which is the fundament to separate single colony from colony clusters using human eyes or computer vision systems. Changes in spectral reading between colony centers and colony edges indicate that spectral features can be employed to separate single colony from colony clusters.

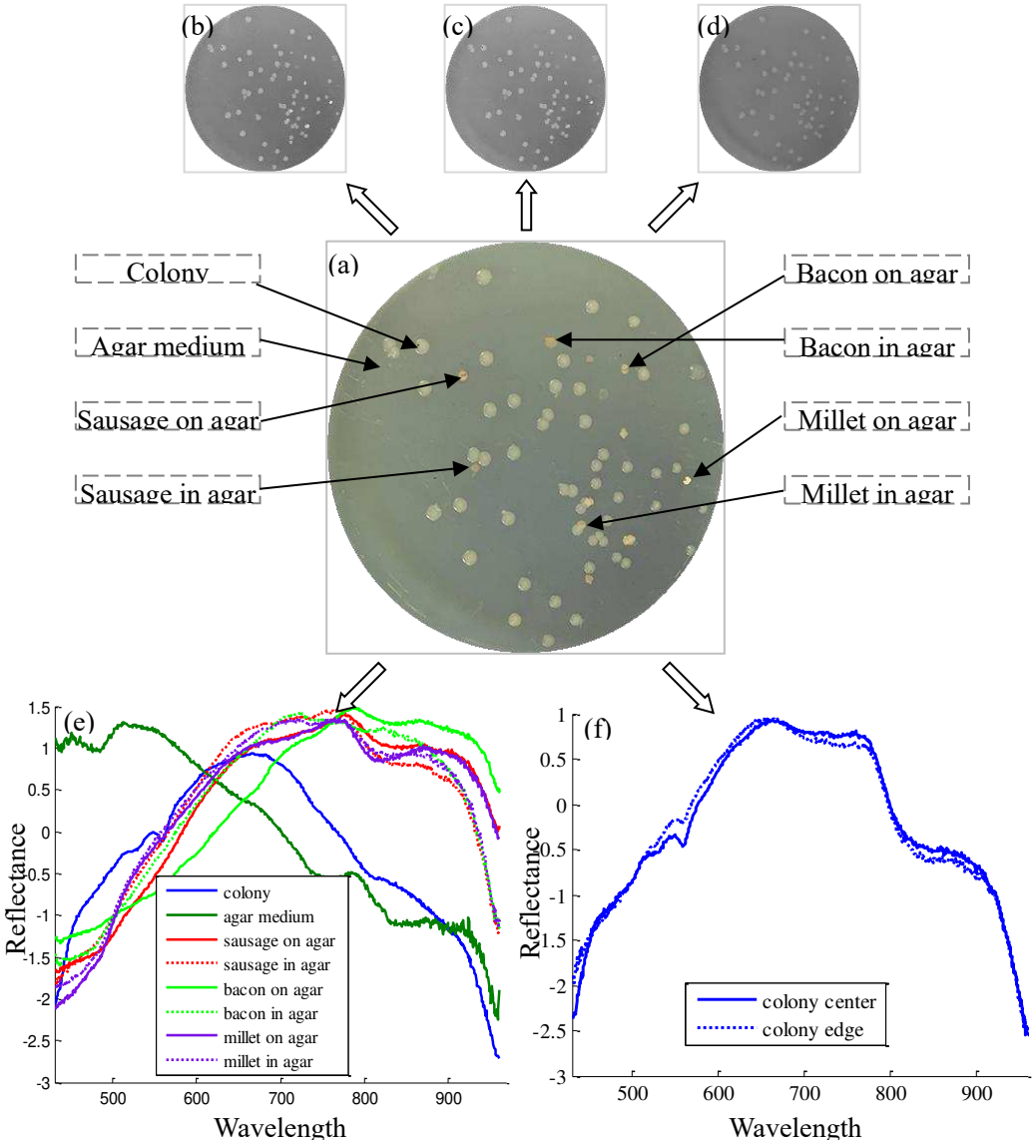

Figure 4 spectral/image features of agar plate. (a) Color image of an agar plate; (b) R gray image of the color image; (c) G gray image of the color image; (d) B gray image of the color image; (e) the mean spectra data of the colonies and non-colonies particles; (f) the mean spectra data of the colony center and colony edge.

3.2 building cluster segmenting calibration model

90 spectrums belonging to colonies, 90 spectrums belonging to food fragments, and 60 spectrums belonging to the agar medium were extracted from the hyperspectral images. Spectrums of colonies were in the foreground category,

297 spectrums of food fragments and agar medium were in the background category. The
298 spectra data of the foreground/background samples and their categories were
299 employed to build colony areas segment model, as described in section 2.4.1.
300 GA, PCA and KNN algorithms were employed to build colony areas
301 segmentation models. In this study, the parameters used in GA algorithm were set as
302 following: number of max generations (*Maxgen*) was equal to 60, crossover
303 probability (*Pc*) was equal to 0.50, mutation probability (*Pm*) was equal to 0.05,
304 population size (*Popsize*) was equal to 60, the length of a chromosome (*Chrolen*) was
305 equal to 40, the average probability of variables selected in chromosomes of the
306 initialized population (*Pinit*) was equal to 10%. The fitness values (*Fvalue*) was the
307 identification rates (*Ir*) of KNN model. Foreground samples were defined as
308 “positives”, and background samples were defined as “negatives”. Details of optimal
309 calibration models with spectra data and chemometrics methods were described in
310 section 2.3.
311 The capability of optimal calibration modes for segmentation of an unknown
312 sample was tested by an independent testing set. So 60 spectrums belonging to
313 colonies, 60 spectrums belonging to food fragments, and 60 spectrums belonging to
314 the agar medium were extracted from the hyperspectral images and used to construct
315 the testing data set. With different spectral treatment, the results of the calibration
316 model were summarized in Table 1. The identification rates of the calibration data set,
317 prediction data set and testing data based on raw spectra were 95.63%, 92.50% and
318 91.67%, respectively. The identification rates of the calibration data set, prediction
319 data set and testing data based on SNV pretreatment were 98.75%, 96.25% and
320 95.56%, respectively. Compared with the raw spectral without any pretreatment, SNV
321 pretreatment can enhance the performance of calibration model, this indicating that
322 the scattering effects and baseline shifts contribute a part of the unwanted variations
323 in the raw spectra.
324 Compared with the results based on SNV pretreatment, the calibration model
325 based on GA wavelength selection got better results. The identification rates of the
326 testing data set based on GA wavelength selection were 99.44%, which means the

calibration model based on GA wavelength gets high capability for segmentation of an unknown sample. The identification results based on GA wavelength selection also indicated that the spectral features corresponding to foreground/background samples were characterized successfully by the optimized identification model.

Table 1 results of the cluster segmenting calibration models

Spectra treatment	Calibration results			Validation results			Testing results						
	Ir	Se	Sp	Ir	Se	Sp	Ir	TP	FN	TN	FP	Se	Sp
Raw spectra	95.63	96.67	95.00	92.50	93.33	92.00	91.67	55	5	110	10	91.67	91.67
SNV pretreatment	98.75	100	98.00	96.25	96.67	96.00	95.56	57	3	115	5	95.00	95.83
GA wavelength selection	100	100	100	100	100	100	99.44	60	0	119	1	100	99.17

3.3 building colony separating calibration model

90 spectrums belonging to colony center regions, and 90 spectrums belonging to colony border regions were extracted from the hyperspectral images. Spectrums of colony center regions were in the foreground category, spectrums of colony border regions were in the background category. The spectra data of the foreground/background samples and their categories were employed to build colony areas segment model, as described in section 2.4.2. Similar to the date processing in section 3.2, the GA, PCA and KNN algorithms were also employed to optimize colony center identification model. The same GA parameters (*Maxgen, Pc, Pm, Popsize, Chrolen, Pinit, Ir, Fvalue*) in Section 3.2 were used in this section. Foreground samples were defined as “positives”, and background samples were defined as “negatives”. Details of optimal calibration models with spectra data and chemometrics methods were described in section 2.3.

The capability of optimal calibration model for segmentation of an unknown sample was also tested by an independent testing set. So 30 spectrums belonging to colony center regions, and 30 spectrums belonging to colony border regions were extracted from the hyperspectral images and used to construct the testing data set.

With different spectral treatment, the results of the calibration model were summarized in Table 2. The identification rates of the calibration data set, prediction data set and testing data based on raw spectra were 92.50%, 90.00% and 88.33%, respectively. The identification rates of the calibration data set, prediction data set and testing data based on SNV pretreatment were 95.00%, 93.33% and 91.67%, respectively. Compared with the results based on raw spectral, the performance of calibration model has been enhanced after SNV pretreatment. The identification rates of the calibration data set, prediction data set and testing data based on GA wavelength selection were 98.33%, 95.00% and 93.33%, respectively. It could be found that the best identification results obtained after GA wavelength selection, which indicated the spectral features corresponding to colony center/border characterized successfully by the optimized identification model.

Table 2 results of the colony separating calibration models

Spectra treatment	Calibration results			Validation results			Testing results						
	Ir	Se	Sp	Ir	Se	Sp	Ir	TP	FN	TN	FP	Se	Sp
Raw spectra	92.50	96.67	88.33	90.00	90.00	90.00	88.33	27	3	26	4	90.00	86.67
SNV pretreatment	95.00	96.67	93.33	93.33	93.33	93.33	91.67	28	2	27	3	93.33	90.00
GA wavelength selection	98.33	100	96.67	95.00	96.67	93.33	93.33	29	1	27	3	96.67	90.00

3.4 count of bacterial colonies

Agar plates with 76 colonies (as shown in Fig. 5 (a)), agar medium, and 13 food fragments in/on agar medium were employed to collect hyperspectral images using the method described in section 2.2. The spectral data of each pixel in the hyperspectral image were extracted and employed for colony count, which mainly include segmentation of colony areas from background, separating single colony from clusters, and colony count, as described in section 2.4.3.

3.4.1 Segmentation of colony areas from the background

After hyperspectral image collection, the hyperspectral image date of the agar plate was obtained as shown in Fig. 5(c). The spectral data of each pixel in the hyperspectral image were employed to segment colony areas from the background. The same spectral features used in the segmenting model were extracted and substituted into the optimal calibration model to predict the category that every pixel belongs to. The gray level of a pixel was set to "1" if the pixel was divided into foreground category (the pixel belongs to colony regions) by the optimal segment model, and the gray level of a pixel was set to "0" if the pixel was divided into background category (the pixel belongs to food fragments or agar medium regions). The binary image of the agar plate after colony segment using the optimal segment model was shown in Fig. 5 (e). The two dimension gray image of the agar plate was collected as shown in Fig. 5(b), and the binary image of the agar plate after colony segment using conventional computer vision with threshold values (150, 200) was also presented in Fig. 5 (d).

In Fig. 5(d), it could be found that 4 food fragments (marked with red square) appear in the foreground region after conventional computer vision processing, which means the four food fragments were wrongly segmented as colonies. This results are caused by that the grayscales of the food fragments are quite close to that of colonies at R, G, B bands, and it is very difficult to set a threshold value to differentiate colonies from food fragments. In Fig. 5(e), it could be found that only colonies appear in the foreground region after colony segment using hyperspectral features, and all the food fragments were identified as background successfully. This results indicated that hyperspectral features are able to differentiate colonies from food fragments even though the color of food fragments are similar to that of colonies.

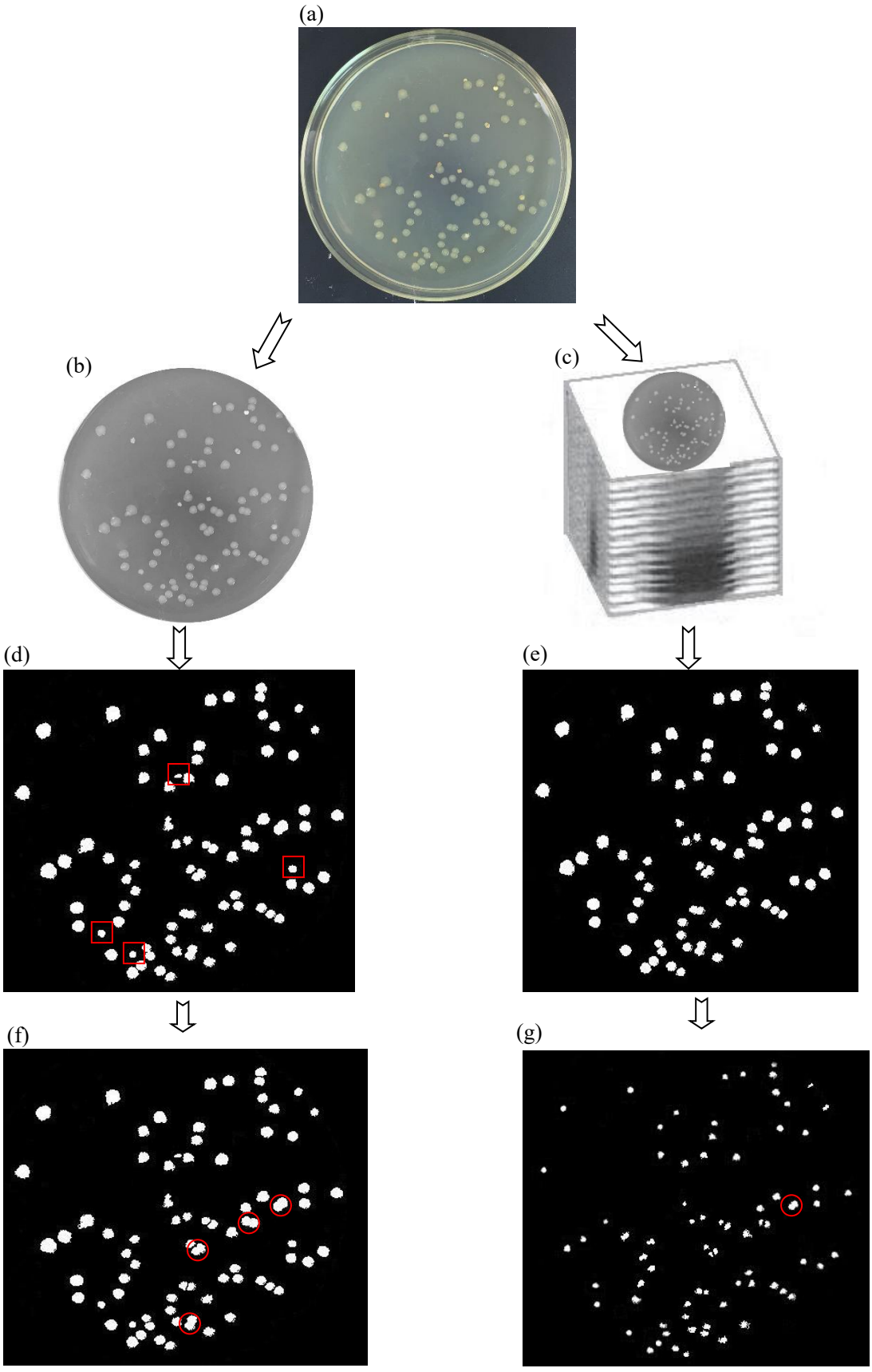

Figure 5 colony count using hyperspectral imaging technology and conventional

computer vision. (a) An agar plate with colonies and food fragments. (b) Gray image data of the agar plate. (c) Hyperspectral image data of the agar plate. (d) The binary image of the agar plate after colony segment using conventional computer vision. (e) The binary image of the agar plate after colony segment using the optimal segment model. (f) The binary image of the touching colonies after colony separation using conventional computer vision. (g) The binary image of the touching colonies after colony separation using colony separating model.

3.4.2 Identification of colonies contacting or overlapping with each other

After colony area segmentation, the spectral data of each pixel in the colony areas were employed to identify colony centers. The same spectral features used in the colony separation model were extracted and substituted into the optimal calibration model to predict the category that every pixel belongs to. The gray level of a pixel was set to "1" if the pixel was divided into foreground category (the pixel belongs to colony center) by the optimal segment model, and the gray level of a pixel was set to "0" if the pixel was divided into background category (the pixel belongs to colony border). The binary image of the agar plate after colony segment using the optimal segment model was shown in Fig. 5 (g). The binary image of the agar plate after colony segment using conventional computer vision with the watershed algorithm was also presented in Fig. 5 (f).

There are 9 colony clusters containing two or three colonies, as shown in Fig. 5(a). In Fig. 5(f), it could be found that colonies in 5 clusters were separated successfully, and 4 clusters (marked with red circle) were wrongly identified as single colonies. This results are caused by that the grayscales of the food fragments are quite close to that of colonies at R, G, B bands, and it is very difficult to set a threshold value to differentiate colonies from food fragments. In Fig. 5(f), it could be found that colonies in 8 clusters were separated successfully, and only one clusters (marked with red circle) was wrongly identified as single colonies. This results indicated that hyperspectral features are more powerful than conventional computer vision in

433 separation colonies in colony clusters.

434

435 3.4.3 Colony count

436 After segmentation of colony areas from the background and identification of
437 colonies contacting or overlapping with each other, colonies on the agar plated can be
438 counted. The spot image of the recognized colonies processed using conventional
439 computer vision was shown in Fig. 5(f), the spot image of the recognized colonies
440 processed using the proposed method based on hyperspectral features was shown in
441 Fig. 5(g). The agar plate (Fig. 5 (a)) were used to determine the reference value of
442 colony number by human vision with a magnifying glass and the reference value of
443 colony number is 76. In Fig. 5(f), the computer vision count error is caused by that 4
444 food fragments were segmented as colonies in Fig. 5(d) and 4 multi-colony clusters
445 were identified as single colonies in Fig. 5(f). In Fig. 5(g), colony number obtained
446 using conventional computer vision is 75, the count error is caused by that 1 multi-
447 colony cluster with two colonies was identified as single colonies in Fig. 5(g).
448 Compared with the conventional computer vision method, the proposed method based
449 on hyperspectral features is more powerful to count colonies on agar plates.

450 The capability of the proposed method for different colony numbers was tested.
451 20 agar plates with various colony concentrations and food fragments were
452 determined using hyperspectral imaging technology, computer vision method and
453 human vision at the same time. The correlation between hyperspectral imaging
454 method and human vision method are shown in Fig. 6. As shown in Fig. 6, an
455 excellent value of correlation efficiency was obtained in the hyperspectral imaging
456 method. The hyperspectral imaging method was demonstrated as a reliable method
457 that can count microbial colonies to the same level as the human vision count method.

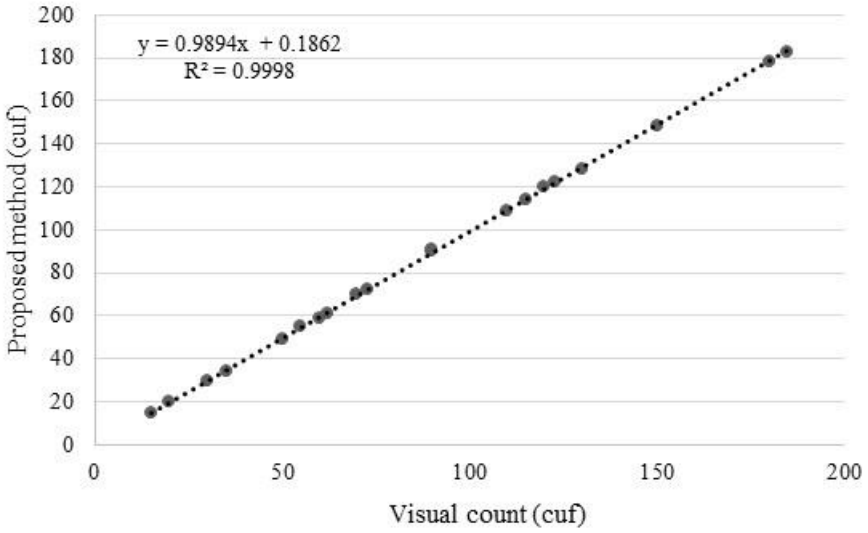

458

459 Figure 6 the correlation of colony count results determined by hyperspectral

460 imaging method and human vision method

461

462 3.5 discussion

463 Errors caused by colony count will be amplified hundred or thousand times in

464 converting colony numbers to the total number of microbial cells in food products, as

465 the extraction of food samples need to be diluted by hundred or thousand times in

466 colony cultivation. The automated colony count method mainly focuses on how to

467 provide reliable results in colony detection. There are some cases in which error occurs

468 during automated colony counting. In the presence of noises caused by various food

469 fragments, the noises maybe identified as normal colony, and the numbers of colonies

470 determined by automated colony count method is higher than the truth value. The

471 microbiological safety risk on food products will be overestimated in this case. In the

472 presence of a cluster comprised multiple colonies, the cluster maybe identified as a

473 single colony, and the numbers of colonies determined by automated colony count

474 method is lower than the truth value. The microbiological safety risk on food products

475 will be underestimated in this case. So distinguishing the colonies from the noise and

476 separation colonies from the cluster are the key steps to ensure the precision of colony

477 counting.

478 Usually, conventional computer vision collects color images of an agar plate, then

colonies were segmented and counted from the background according to colors/shapes features. Conventional computer vision is effective to agar plates with high gray contrast between colony and its background, or without food fragments producing noises in color images. The proposed method extract spectral features of colony and its background to segment and count colonies, so it presented good performance in identifying food fragments with similar color/shapes to colonies, or separating single colony from clusters. As researches in school and technicians in government institution of Disease Control and Prevention reported that food fragments appear at/in agar medium frequently. Compared with conventional computer vision, the proposed method could produce more reliable results in practice for food quality assessment.

Complex chemometrics methods are necessary in building calibration models, which makes the data processing complex, while the data processing in colony count using the established calibration models is quite simple in the proposed method. Usually, wavelength selection chemometrics methods are employed to select the most informative wavelengths correlating with the samples and pattern recognition chemometrics methods are employed to establish the correlation ships between selected spectra data (or spectral features) and sample qualities. These data processing in building calibration models can't be skipped due to the complex interaction between detecting lights and food samples. However, the use of the established calibration models for predicting sample qualities is very simple. As the step 3 in Fig. 3, the main data processing for colony count includes extract spectral features from the raw data and substitute the spectral features to the established calibration models. The data processing can be completed using an ordinary computer without any chemometrics procedures.

4 conclusion

A new noise free method was proposed to count microbial colonies for food quality assessment using hyperspectral imaging technology. Agar plates with microbial colonies and various food fragments with similar colors/shapes to colonies were employed to collect hyperspectral image data. The spectral features of

colonies/food fragments, colony centers/borders were extracted from the hyperspectral images and employed to build calibration models for segmenting colonies from the background, separating single colony from clusters. With the aid of the calibration models, each pixel of an agar plate hyperspectral image can be identified according to their spectral features. Results shown that the proposed method got good correlation (R^2= 0.9998) with human vision method widely employed as national standards. Compared with conventional computer vision method, the proposed method is effective to identify the noised caused by food fragments with similar colors/shapes to colonies. It could be concluded that the proposed method can detect microbial colonies to the same level as the standard method and is therefore of practical importance.

Acknowledgements

The authors gratefully acknowledge the financial support provided by the National Key Research and Development Program of China (2016YFD0401104), the National Natural Science Foundation of China (31772073, 31671844), the Natural Science Foundation of Jiangsu Province (BK20160506, BE2016306), International Science and Technology Cooperation Project of Jiangsu Province (BZ2016013), Suzhou Science and Technology Project (SNG201503), China Postdoctoral Science Foundation (2016M600379, 2016M590422, 2017T100334), Natural Science Foundation of the Jiangsu Higher Education Institutions of China (16KJB550002), Jiangsu Planned Projects for Postdoctoral Research Funds (1601080B), Six Talent Peaks Project in Jiangsu Province (GDZB-016), and Priority Academic Program Development of Jiangsu Higher Education Institutions (PAPD).

References:

1. J. E. L. Corry, B. Jarvis and A. J. Hedges, Food Microbiology, 2010, **27**, 598-603.
2. P. Chiang, M. Tseng, Z. He and C. Li, Journal of Microbiological Methods, 2015, **108**, 74-82.
3. M. M. Lobete, E. N. Fernandez and J. F. M. Van Impe, Frontiers in Microbiology, 2015, **6**.
4. S. Piepers, P. Zrimsek, P. Passchyn and S. De Vliegher, Journal of Dairy Science, 2014, **97**, 3409-

3419.
5. F. Feroz, H. Shimizu, T. Nishioka, M. Mori and Y. Sakagami, Biocontrol Science, 2016, **21**, 243-251.
6. D. Rysanek, M. Zouharova and V. Babak, Journal of Dairy Research, 2009, **76**, 117-123.
7. AOAC 966.23.C Microbiological Methods/Aerobic Plate Count. 1989.
8. American Public Health Association. Standard Methods for the Examination of Dairy Products, 16th ed. 1993..
9. National Health and Family planning Commission of the People's Republic of China, China Food and Drug Administration, national food safety standards: food microbiological analysis-Aerobic Plate Count, GB4789.2-2016.
10. A. Ferrari, S. Lombardi and A. Signoroni, Pattern Recognition, 2017, **61**, 629-640.
11. J. Dahle, M. Kakar, H. B. Steen and O. Kaalhus, Cytometry Part a, 2004, **60A**, 182-188.
12. W. Chen and C. Zhang, Information Systems Frontiers, 2009, **11**, 349-368.
13. E. O. Puchkov, Microbiology, 2010, **79**, 141-146.
14. E. Araki, T. Matsuzaki, T. Sekita, M. Saito and H. Matsuoka, Biocontrol Science, 2010, **15**, 39-43.
15. E. Li, Chinese Journal of Health Laboratory Technology, 2010, **20**, 1940-1941.
16. H. Ogawa, S. Nasu, M. Takeshige, H. Funabashi, M. Saito and H. Matsuoka, Journal of Microbiological Methods, 2012, **91**, 420-428.
17. M. L. Clarke, R. L. Burton, A. N. Hill, M. Litorja, M. H. Nahm and J. Hwang, Cytometry Part a, 2010, **77**, 790-797.
18. G. Wei, Fujian Analysis &Testing, 2008, **17**, 32-35.
19. Y. Tang, J. Lan, X. Gao, X. Liu, D. Zhang, L. Wei, Z. Gao and J. Li, Food Chemistry, 2016, **190**, 952-959.
20. Y. Bao, F. Liu, W. Kong, D. Sun, Y. He and Z. Qiu, Food and Bioprocess Technology, 2014, **7**, 54-61.
21. J. Li, W. Huang, C. Zhao and B. Zhang, Journal of Food Engineering, 2013, **116**, 324-332.
22. B. G. Botelho, N. Reis, L. S. Oliveira and M. M. Sena, Food Chemistry, 2015, **181**, 31-37.
23. L. Du, W. Gong, S. Shi, P. Yang, J. Sun, B. Zhu and S. Song, International Journal of Applied Earth Observation and Geoinformation, 2016, **44**, 136-143.
24. H. He, D. Wu and D. Sun, Journal of Food Engineering, 2014, **126**, 156-164.
25. Y. Zhu, X. Zou, T. Shen, J. Shi, J. Zhao, M. Holmes and G. Li, Journal of Food Engineering, 2016, **174**, 75-84.
26. J. Shi, X. Zou, J. Zhao, K. Wang, Z. Chen, X. Huang, D. Zhang and M. Holmes, Scientia Horticulturae, 2012, **138**, 190-197.
27. J. Shi, X. Zou, J. Zhao and X. Yin, Chinese Journal of Analytical Chemistry, 2011, **39**, 243-247.
28. J. Cheng and D. Sun, Food and Bioprocess Technology, 2015, **8**, 951-959.
29. J. Cheng, D. Sun, H. Pu, Q. Wang and Y. Chen, Food Chemistry, 2015, **171**, 258-265.
30. X. B. Zou, J. Y. Shi, H. L. Min, J. W. Zhao, H. P. Mao, Z. W. Chen, Y. X. Li and H. Mel, Analytica Chimica Acta, 2011, **706**, 105-112.
31. X. B. Zou, J. W. Zhao, M. Povey, M. Holmes and H. P. Mao, Analytica Chimica Acta, 2010, **667**, 14-32.
32. M. Arakawa, Y. Yamashita and K. Funatsu, Journal of Chemometrics, 2011, **25**, 10-19.
33. J. Y. Shi, X. B. Zou, J. W. Zhao and M. Holmes, Journal of Near Infrared Spectroscopy, 2012, **20**, 295-305.
34. F. Vogt and M. Tacke, Chemometrics and Intelligent Laboratory Systems, 2001, **59**, 1-18.

35. X. B. Zou, J. W. Zhao, M. Holmes, H. P. Mao, J. Y. Shi, X. P. Yin and Y. X. Li, Chemometrics and Intelligent Laboratory Systems, 2010, **104**, 265-270.
36. R. Moscetti, R. P. Haff, E. Stella, M. Contini, D. Monarca, M. Cecchini and R. Massantini, Postharvest Biology and Technology, 2015, **99**, 58-62.
37. T. T. Shen, X. B. Zou, J. Y. Shi, Z. H. Li, X. W. Huang, Y. W. Xu and W. Chen, Food Analytical Methods, 2016, **9**, 68-79.
38. L. Xu and X. Shao (2004) *Method of chemometrics*. Science Press of China, Beijing.

校对报告

当前使用的样式是 [Analytical Methods New]
当前文档包含的题录共40条
有0条题录存在必填字段内容缺失的问题
所有题录的数据正常